

Audiovisual SlowFast Networks for Video Recognition

Fanyi Xiao^{1,2*} Yong Jae Lee¹ Kristen Grauman² Jitendra Malik² Christoph Feichtenhofer²

¹University of California, Davis

²Facebook AI Research (FAIR)

Abstract

We present *Audiovisual SlowFast Networks*, an architecture for integrated audiovisual perception. AVSlowFast has Slow and Fast visual pathways that are deeply integrated with a Faster Audio pathway to model vision and sound in a unified representation. We fuse audio and visual features at multiple layers, enabling audio to contribute to the formation of hierarchical audiovisual concepts. To overcome training difficulties that arise from different learning dynamics for audio and visual modalities, we introduce *DropPathway*, which randomly drops the Audio pathway during training as an effective regularization technique. Inspired by prior studies in neuroscience, we perform hierarchical audiovisual synchronization to learn joint audiovisual features. We report state-of-the-art results on six video action classification and detection datasets, perform detailed ablation studies, and show the generalization of AVSlowFast to learn self-supervised audiovisual features. Code will be made available at: <https://github.com/facebookresearch/SlowFast>.

1. Introduction

Joint audiovisual learning is core to human perception. However, most contemporary models for video analysis exploit only the visual signal and ignore the audio signal. For many video understanding tasks, audio could be very helpful. Audio has the potential to influence action recognition not only in obvious cases where sound dominates, like “playing saxophone”, but also visually subtle cases where the action itself is difficult to see in the video frames, like “whistling”, or closely related actions where sound helps disambiguate, like “closing” vs. “slamming” the door.

This line of thinking is supported by perceptual and neuroscience studies suggesting interesting ways in which visual and audio signals are combined in the brain. A classic example is the McGurk effect [53]¹ – when one is listening to an audio clip (e.g., sounding “ba-ba”), alongside watching a video of fabricated lip movements (indicating “va-va”), the sound one perceives *changes* (in this case from “ba-ba” to “va-va”).

*Work done during an internship at Facebook AI Research.

¹<https://www.youtube.com/watch?v=G-1N8vWm3m0>

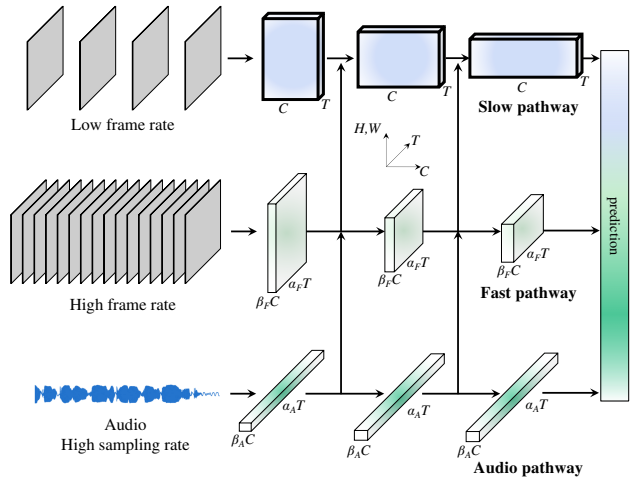


Figure 1. **Audiovisual SlowFast Networks** have Slow and Fast visual pathways that are deeply integrated with a Faster Audio pathway to model vision and sound in a unified representation.

This effect demonstrates that there is tight entanglement between audio and visual signals (known as the *multisensory integration process*) [52, 42, 71, 70]. Importantly, research has suggested this fusion between audio and visual signals happens at a fairly early stage [64, 57].

Given its high potential in facilitating video understanding, researchers have attempted to utilize audio in videos [41, 24, 2, 5, 58, 59, 3, 65, 23]. However, there are a few challenges in making effective use of audio. First, audio does not always correspond to the visual frames (e.g., in a “dunking basketball” video, there can be class-unrelated background music playing). Conversely, audio does not always contain information that can help understand the video (e.g., “shaking hands” does not have a particular sound signature). There are also challenges from a technical perspective. Specifically, we identify the incompatibility of “learning dynamics” between the visual and audio pathways – audio pathways generally train much faster than visual ones, which can lead to generalization issues during joint audiovisual training. Due in part to these various difficulties, a principled approach for audiovisual modeling is currently lacking. Many previous methods adopt an ad-hoc scheme that consists of a separate audio network that is integrated with the visual pathway via “late-fusion” [24, 2, 58].

The objective of this paper is to build an architecture for *integrated audiovisual perception*. We aim to go beyond previous work that performs “late-fusion” of independent audio and visual pathways, to instead learn *hierarchies* of integrated audiovisual features, enabling unified audiovisual perception. We propose a new architecture, *Audiovisual SlowFast Networks* (AVSlowFast), to perform fusion at multiple levels (Fig. 1). AVSlowFast Networks build on SlowFast [16], a class of architectures that has two pathways, of which one (Slow) is designed to capture more static but semantic-rich information whereas the other (Fast) is tasked to capture motion. AVSlowFast hierarchically intertwines a Faster Audio pathway with the Slow and Fast pathways, as audio has higher sampling rate, that learns end-to-end from vision and sound. The Audio pathway can be lightweight (<20% of computation), but requires a careful design and training strategies to be useful in practice.

We evaluate our approach on standard datasets in the human action recognition community and find consistent improvement for integrating audio. The improvement in accuracy varies for datasets and classes but comes with a relatively small increase in computational cost. For example, on the leading dataset for egocentric video, EPIC-kitchens [14], audio boosts by +2.9/+4.3/+2.3 the top-1 accuracy for verb/noun/action recognition at 20% of overall compute, on Kinetics [40] action classification by +1.4 top-1 accuracy at 11% of compute, and on AVA [28] action detection by +1.2 mAP at only 2% of the overall compute.

Our key contributions are:

(i) We present AVSlowFast, which fuses audio and visual information *at multiple levels* in the network hierarchy (*i.e.*, hierarchical fusion) so that audio can contribute to the formation of visual concepts at different levels of abstraction. In contrast to late-fusion, this enables the audio signal to participate in the process of forming visual features.

(ii) To overcome the incompatibility of learning dynamics between the visual and audio pathways, we propose *DropPathway*, which randomly drops the Audio pathway during training as a simple and effective regularization technique to tune the pace of the learning process. This enables us to train our joint audiovisual model with hierarchical fusion connections across modalities.

(iii) Inspired by the multisensory integration process mentioned above and prior work in neuroscience [42], which suggests that there exist *audiovisual mirror neurons* in monkey brains that respond to “any evidence of the action, be it auditory or visual”, we propose to perform audio visual synchronization (AVS) [58, 45, 2, 5] at multiple layers to learn features that generalize across modalities.

(iv) We conduct extensive experiments on six video recognition datasets for human action classification and detection. We report state-of-the-art results and provide ablation studies to understand the trade-offs of various de-

sign choices. In addition to evaluating the performance of AVSlowFast for established supervised video classification and detection tasks, we validate the generalization of the audiovisual representation to self-supervised learning, revealing that strong video features can be learned with AVSlowFast using standard pretraining objectives.

2. Related Work

Video recognition. Significant progress has been made in video recognition in recent years. Some notable directions are two-stream networks in which one stream processes RGB frames and the other processes optical flow [67, 17, 79], 3D ConvNets as an extension of 2D networks to the spatiotemporal domain [76, 61, 84], and recent SlowFast Networks that have two pathways to process videos at different temporal frequencies [16]. Despite all these efforts on harnessing temporal information in videos, research is relatively lacking when it comes to another important information source – audio in video.

Audiovisual activity recognition. Joint modeling of audio and visual signals has been largely conducted in a “late-fusion” manner in video recognition literature [41, 50, 24]. For example, all the entries that utilize audio in the 2018 ActivityNet challenge report [24] have adopted this paradigm – meaning that there are networks processing visual and audio inputs separately, and then they either concatenate the output features or average the final class scores across modalities. Recently, an interesting audiovisual fusion approach has been proposed [41] using flexible binding windows when fusing audio and visual features. With three similar network streams, this approach fuses audio features with the features from RGB and optical flow at the final stage before classification. In contrast, AVSlowFast is building a hierarchically integrated audiovisual representation.

Multi-modal learning. Researchers have long been interested in developing models that can learn from multiple modalities (e.g., audio, vision, language). Beyond audio and visual modalities, extensive research has been conducted in other instantiations of multi-modal learning, including vision and language [20, 4, 83], vision and locomotion [87, 22], and learning from physiological data [48].

Other audiovisual tasks. Audio has also been extensively utilized outside of video recognition, *e.g.* for learning audiovisual representations in a self-supervised manner [2, 5, 58, 59, 45, 34] by exploiting audio-visual correspondence. Other audiovisual tasks include audio-visual speech recognition [60, 56], lip reading [12], biometric matching [55], sound-source localization [10, 3, 65, 86, 34, 15], audiovisual source separation [58, 23], and audiovisual question answering [1].

3. Audiovisual SlowFast Networks

Inspired by research in neuroscience [7], which suggests that audio and visual signals fuse at multiple levels, we propose to fuse audio and visual features at multiple stages, from intermediate-level features to high-level semantic concepts. This way, audio can participate in the formation of visual concepts at different levels. AVSlowFast Networks are conceptually simple: SlowFast has Slow and Fast pathways to process visual input (§3.1), and AVSlowFast extends this with an Audio pathway (§3.2).

3.1. SlowFast pathways

We begin by briefly reviewing the SlowFast architecture [16]. The Slow pathway (Fig. 1, top row) is a convolutional network that processes videos with a large temporal stride (*i.e.*, it samples one frame out of τ frames). The primary goal of the Slow pathway is to produce features that capture semantic contents of the video, which has a low refresh rate (semantics do not change all of a sudden). The Fast pathway (Fig. 1, middle row) is another convolutional model with three key properties. First, it has an α_F times higher frame rate (*i.e.*, with temporal stride τ/α_F , $\alpha_F > 1$) so that it can capture fast motion information. Second, it preserves fine temporal resolution by avoiding any temporal downsampling. Third, it has a lower channel capacity (β_F times the Slow pathway channels, where $\beta_F < 1$) as it is demonstrated to be a desired trade-off [16]. We refer readers to [16] for more details.

3.2. Audio pathway

A key property of the Audio pathway is that it has an even finer temporal structure than the Slow and Fast pathways (with waveform sampling rate on the order of kHz). As standard processing, we take a log-mel-spectrogram (2-D representation in time and frequency of audio) as input and set the temporal stride to τ/α_A frames, where α_A can be much larger than α_F (*e.g.*, 32 *vs.* 8). In a sense, it serves as a “Faster” pathway with respect to Slow and Fast pathways. Another notable property of the Audio pathway is its low computation cost, as audio signals, due to their lower-dimensional nature, are cheaper to process than visual signals. To control this, we set the channels of the Audio pathway to $\beta_A \times$ Slow pathway channels. By default, we set β_A to 1/2. Depending on the specific instantiation, the Audio pathway typically only requires 10% to 20% of the overall computation of AVSlowFast.

3.3. Lateral connections

In addition to the lateral connections between the Slow and Fast pathways in [16], we add lateral connections between the Audio, Slow, and Fast pathways to fuse audio and visual features. Following [16], lateral connections are

stage	Slow pathway	Fast pathway	Audio pathway
raw clip	$3 \times 64 \times 224^2$	$3 \times 64 \times 224^2$	80×128 (<i>freq. \times time</i>)
data layer	stride 16, 1^2	stride 2, 1^2	-
conv ₁	1×7^2 , 64 stride 1, 2^2	5×7^2 , 8 stride 1, 2^2	$[9 \times 1, 1 \times 9]$, 32 stride 1, 1
pool ₁	1×3^2 max stride 1, 2^2	1×3^2 max stride 1, 2^2	-
res ₂	$\begin{bmatrix} 1 \times 1^2, 64 \\ 1 \times 3^2, 64 \\ 1 \times 1^2, 256 \end{bmatrix} \times 3$	$\begin{bmatrix} 3 \times 1^2, 8 \\ 1 \times 3^2, 8 \\ 1 \times 1^2, 32 \end{bmatrix} \times 3$	$\begin{bmatrix} 1 \times 1, 32 \\ [3 \times 1, 1 \times 3], 32 \\ 1 \times 1, 128 \end{bmatrix} \times 3$
res ₃	$\begin{bmatrix} 1 \times 1^2, 128 \\ 1 \times 3^2, 128 \\ 1 \times 1^2, 512 \end{bmatrix} \times 4$	$\begin{bmatrix} 3 \times 1^2, 16 \\ 1 \times 3^2, 16 \\ 1 \times 1^2, 64 \end{bmatrix} \times 4$	$\begin{bmatrix} 1 \times 1, 64 \\ [3 \times 1, 1 \times 3], 64 \\ 1 \times 1, 256 \end{bmatrix} \times 4$
res ₄	$\begin{bmatrix} 3 \times 1^2, 256 \\ 1 \times 3^2, 256 \\ 1 \times 1^2, 1024 \end{bmatrix} \times 6$	$\begin{bmatrix} 3 \times 1^2, 32 \\ 1 \times 3^2, 32 \\ 1 \times 1^2, 128 \end{bmatrix} \times 6$	$\begin{bmatrix} 1 \times 1, 128 \\ 3 \times 3, 128 \\ 1 \times 1, 512 \end{bmatrix} \times 6$
res ₅	$\begin{bmatrix} 3 \times 1^2, 512 \\ 1 \times 3^2, 512 \\ 1 \times 1^2, 2048 \end{bmatrix} \times 3$	$\begin{bmatrix} 3 \times 1^2, 64 \\ 1 \times 3^2, 64 \\ 1 \times 1^2, 256 \end{bmatrix} \times 3$	$\begin{bmatrix} 1 \times 1, 256 \\ 3 \times 3, 256 \\ 1 \times 1, 1024 \end{bmatrix} \times 3$

global average pool, concat, fc

Table 1. **An instantiation of the AVSlowFast network.** For Slow & Fast pathways, the dimensions of kernels are denoted by $\{T \times S^2, C\}$ for temporal, spatial, and channel sizes. For the Audio pathway, kernels are denoted with $\{F \times T, C\}$, where F and T are frequency and time. Strides are denoted with $\{\text{temporal stride, spatial stride}^2\}$ and $\{\text{frequency stride, time stride}\}$ for SlowFast and Audio pathways, respectively. The speed ratios are $\alpha_F = 8$, $\alpha_A = 32$ and the channel ratios are $\beta_F = 1/8$, $\beta_A = 1/2$ and $\tau = 16$. The backbone is ResNet-50.

added after ResNet “stages” (*e.g.*, pool₁, res₂, res₃, res₄ and pool₅). However, unlike [16], which has lateral connections after each stage, we found that it is most beneficial to have lateral connections between audio and visual features starting from intermediate levels (we ablate this in Sec. 4.2). This is conceptually intuitive as very low-level visual features such as edges and corners might not have a particular sound signature. Next, we discuss several concrete AVSlowFast instantiations.

3.4. Instantiations

AVSlowFast Networks define a generic class of models that follow the same design principles. In this section, we exemplify a specific instantiation in Table 1. We denote spatiotemporal size by $T \times S^2$ for Slow/Fast pathways and $F \times T$ for the Audio pathway, where T is the temporal length, S is the height and width of a square spatial crop, and F is the number of frequency bins for audio.

SlowFast pathways. For Slow and Fast pathways, we follow the basic instantiation of SlowFast 4×16 , R50 model defined in [16]. It has a Slow pathway that samples $T = 4$ frames out from a 64-frame raw clip with a temporal stride $\tau = 16$. There is no temporal downsampling in the Slow pathway, since input stride is large. Also, it only applies non-degenerate temporal convolutions (temporal stride > 1) in res₄ and res₅ (see Table 1), as this is more effective.

For the Fast pathway, it has a higher frame rate ($\alpha_F = 8$) and a lower channel capacity ($\beta_F = 1/8$), such that it can better capture motion while trading off model capacity. To preserve fine temporal resolution, the Fast pathway has non-degenerate temporal convolutions in every residual block. Spatial downsampling is performed with stride 2^2 convolution in the center (“bottleneck”) filter of the first residual block in each stage of both the Slow and Fast pathways.

Audio pathway. The Audio pathway takes as input the log-mel-spectrogram representation, which is a 2-D representation with one axis being time and the other one denoting frequency bins. In Table 1, we use 128 spectrogram frames (corresponding to 2 seconds of audio) with 80 bins.

Similar to the Slow and Fast pathways, the Audio pathway is also based on a ResNet, but with specific design to better fit the audio inputs. First, we do not pool after the initial convolutional filter (*i.e.* there is no downsampling layer at stage pool₁) to preserve information along both temporal and frequency axis. Downsampling in time-frequency space is performed by stride 2^2 convolution in the center (“bottleneck”) filter of the first residual block in each stage from res₂ to res₅. Second, we decompose the 3×3 convolution filters in res₂ and res₃ into 1×3 filters for frequency and 3×1 filters for time. This increases accuracy slightly (by 0.2% on Kinetics) but also reduces computation. Conceptually, it allows the network to treat time and frequency separately (as opposed to 3×3 filters which imply both axes are uniform) in early stages. While for spatial filters it is reasonable to perform filtering in x and y dimensions symmetrically, this might not be optimal for early filtering in time and frequency dimensions, as the statistics of spectrograms are different from natural images, which instead are approximately isotropic and shift-invariant [63, 35].

Lateral connections. There are many options for how to fuse audio features into the visual pathways. Here, we describe several instantiations and the motivation behind them. Note that this section discusses the lateral connections between the Audio and SlowFast pathways. For the fusion connection between the two visual pathways (Slow and Fast), we adopt the temporal strided convolution as it is demonstrated to be most effective in [16].

(i) $A \rightarrow F \rightarrow S$: In this approach (Fig. 2 left), the Audio pathway (A) is first fused to the Fast pathway (F), and then fused to the Slow pathway (S). Specifically, audio features are subsampled to the temporal length of the Fast pathway and then fused into the Fast pathway with a *sum* operation. After that, the resulting features are further subsampled by α_F (e.g., $4 \times$ subsample) and fused with the Slow pathway (as is done in SlowFast). The key property of this approach is that it enforces *strong temporal alignment* between audio and visual features, as audio features are fused into the Fast pathway which preserves fine temporal resolution.

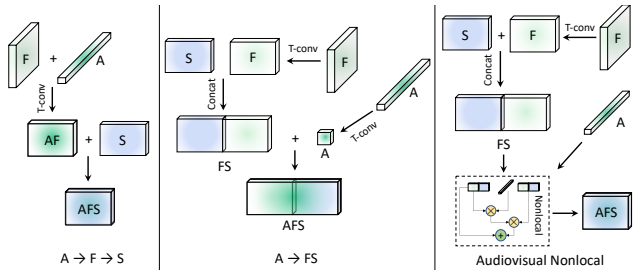


Figure 2. **Fusion connections for AVSlowFast.** *Left:* $A \rightarrow F \rightarrow S$ enforces strong temporal alignment between audio and RGB frames, as audio is fused into the Fast pathway with fine temporal resolution. *Center:* $A \rightarrow FS$ has higher tolerance on temporal misalignment as audio is fused into the temporally downsampled output of SlowFast fusion. *Right:* Audiovisual Nonlocal fuses through a Nonlocal block [80], such that audio features are used to select visual features that are deemed important by audio.

(ii) $A \rightarrow FS$: An alternative way is to fuse the Audio pathway into the output of the SlowFast fusion (Fig. 2 center), which is coarser in temporal resolution. We adopt this design as our default choice as it imposes a less stringent requirement on temporal alignment between audio and visual features, which we found to be important in our experiments. Similar ideas of relaxing the alignment requirement are also explored in [41], in the context of combining RGB, flow, and audio streams.

(iii) Audiovisual Nonlocal: One might also be interested in using audio as a *modulating signal* to visual features. Specifically, instead of directly summing or concatenating audio features into the visual stream, one might expect audio to play a more subtle role of modulating the visual concepts, through attention mechanisms such as Non-Local (NL) blocks [80]. One example would be audio serving as a probing signal indicating where the interesting event is happening in the video, both spatially and temporally, and then focusing the attention of visual pathways on those locations. To materialize this, we adapt NL blocks to take both audio and visual features as inputs (Fig. 2 right). Audio features are then matched to different locations within visual features (along H , W and T axis), and the affinity is used to generate a new visual feature that combines information from locations deemed important by audio features.

3.5. Joint audiovisual training

Unlike SlowFast, AVSlowFast trains with multiple modalities. As noted in Sec. 1, this leads to challenging training dynamics (*i.e.*, different training speed of audio and visual pathways). To tackle this, we propose two training strategies that enable joint training.

DropPathway. We discuss a possible reason for why previous methods employ audio in a late fusion approach. By analyzing the model training dynamics we observe the following. Audio and visual pathways are very different in terms of their “learning speed”.

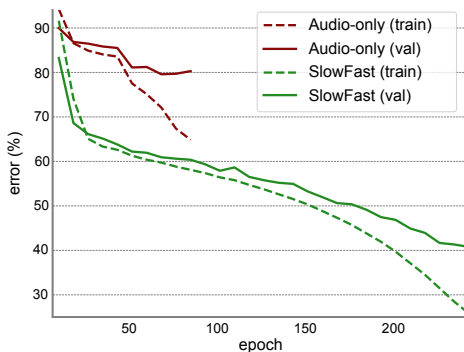


Figure 3. Training procedure on Kinetics for Audio-only (red) vs. SlowFast (green) networks. We show the top-1 training error (dash) and validation error (solid). The curves show single-crop errors; the video accuracy is 24.8% vs. 75.6%. The audio network converges after around $3\times$ fewer iterations compared to the visual.

Taking the curves in Fig. 3 as an example, the green curve is for training a visual-only SlowFast model, whereas the red curve is for training an Audio-only model. It shows that the Audio-only model requires fewer training iterations before it starts to overfit (at ~ 70 epochs, which is $\sim 1/3$ of the visual model’s training epochs). One modality dominating multi-modal training has also been observed for lip-reading applications [12] and optical flow streams in action recognition [18] and video object segmentation [85].

The discrepancy on learning pace leads to overfitting if we naively train both modalities jointly. To unlock the potential of joint training, we propose a simple strategy of randomly dropping the Audio pathway during training (*DropPathway*). Specifically, at each training iteration, we drop the Audio pathway altogether with probability P_d . This way, we *slow down* the learning of the Audio pathway and make its learning dynamics more compatible with its visual counterpart. When dropping the audio pathway, we sum zero tensors with the visual pathways (we also explored feeding the running average of audio features, and found similar results, possibly due to BN).

Our ablation studies in the next section will show the effect of *DropPathway*, showing that this simple strategy provides good generalization and is essential for jointly training AVSlowFast. Note that *DropPathway* is different from simply setting different learning rates for the audio/visual pathways in that it 1) ensures the Audio pathway has fewer parameter updates, 2) hinders the visual pathway to ‘shortcut’ training by memorizing audio information, and 3) provides extra regularization as different audio clips are dropped in each epoch.

Hierarchical audiovisual synchronization. As noted in Sec. 2, temporal synchronization (that comes for free) between audio and visual sources has been explored as a self-supervisory signal to learn feature representations [59, 5, 2, 13, 58, 45, 29]. In this work, we use audiovisual synchronization to encourage the network to produce feature repre-

sentations that are generalizable across modalities (inspired by the *audiovisual mirror neurons* in primate vision [42]). Specifically, we add an auxiliary task to classify whether a pair of audio and visual frames are *in-sync* or not [45, 58] and adopt a curriculum schedule used in [45] that starts with easy negatives (audio and visual frames come from different clips), and transition into a mix of easy and hard (audio and visual frames are from the same clip, but with a temporal shift) after 50% of training epochs. In our experiments, we study the effect of audiovisual synchronization for both supervised and self-supervised audiovisual feature learning.

4. Experiments: Action Classification

We evaluate our approach on six video recognition datasets using standard evaluation protocols. For the action classification experiments in this section we use EPIC-Kitchens [14], Kinetics-400 [40], and Charades [66]. For action detection, we use the AVA dataset [28] covered in Sec. 5, and the AVSlowFast self-supervised representation is evaluated on UCF101 [69] & HMDB51 [47] in Sec. 6.

Datasets. The EPIC-Kitchens dataset [14] consists of daily activities captured in various kitchen environments with egocentric video and sound recordings. It has 39k segments in 432 videos. For each segment, the task is to predict a verb (*e.g.*, “turn-on”), a noun (*e.g.*, “switch”), and an action by combining the two (“turn on switch”). Performance is measured as top-1 and top-5 accuracy. We use the train/val split in [6]. Test results are obtained from the evaluation server.

Kinetics-400 [40] (abbreviated as K400) is a large-scale video dataset of $\sim 240k$ training videos and 20k validation videos in 400 action categories. Results on Kinetics are reported as top-1 and top-5 classification accuracy (%).

Charades [66] is a dataset of $\sim 9.8k$ training videos and 1.8k validation videos in 157 classes. Each video has multiple labels of activities spanning ~ 30 seconds. Performance is measured in mean Average Precision (mAP).

Audio pathway. Following previous work [2, 3, 45, 46], we extract log-mel-spectrograms from the raw audio waveform to serve as the input to Audio pathway. Specifically, we sample audio data with 16 kHz sampling rate, then compute a spectrogram with window size of 32ms and step size of 16ms. The length of the audio input is exactly matched to the duration spanned by the RGB frames. For example, under 30 FPS, for AVSlowFast with $T \times \tau = 8 \times 8$ frames (2 secs) input, we sample 128 frames (2 secs) in log-mel.

Training. We train our AVSlowFast models on Kinetics from scratch without pre-training. We use synchronous SGD and follow the training recipe (learning rate, weight decay, warm-up) used in [16]. Given a training video, we randomly sample T frames with stride τ and extract the corresponding log-mel-spectrogram. We randomly crop 224×224 pixels from a video, randomly flip horizontally, and resize it to a shorter side sampled in [256, 320].

model	verbs		nouns		actions	
	top-1	top-5	top-1	top-5	top-1	top-5
validation						
3D CNN [82]	49.8	80.6	26.1	51.3	19.0	37.8
LFB [82]	52.6	81.2	31.8	56.8	22.8	41.1
SlowFast [16]	55.8	83.1	27.4	52.1	21.9	39.7
AVSlowFast	58.7	83.6	31.7	58.4	24.2	43.6
Δ	+2.9	+0.5	+4.3	+6.3	+2.3	+3.9
test s1 (seen)						
HF-TSN [73]	57.6	87.8	39.9	65.4	28.1	48.6
RU-LSTM [21]	56.9	85.7	43.1	67.1	33.1	55.3
FBK-HUPBA [72]	63.3	89.0	44.8	69.9	35.5	57.2
LFB [82]	60.0	88.4	45.0	71.8	32.7	55.3
EPIC-Fusion [41]	64.8	90.7	46.0	71.3	34.8	56.7
AVSlowFast	65.7	89.5	46.4	71.7	35.9	57.8
test s2 (unseen)						
HF-TSN [73]	42.4	75.8	25.2	49.0	16.9	33.3
RU-LSTM [21]	43.7	73.3	26.8	48.3	19.5	37.2
FBK-HUPBA [72]	49.4	77.5	27.1	52.0	20.3	37.6
LFB [82]	50.9	77.6	31.5	57.8	21.2	39.4
EPIC-Fusion [41]	52.7	79.9	27.9	53.8	19.1	36.5
AVSlowFast	55.8	81.7	32.7	58.9	24.0	43.2
Δ	+3.1	+1.8	+4.8	+4.9	+2.3	+6.7

Table 2. **EPIC-Kitchens validation and test results.** Models pre-train on Kinetics [16, 41, 82] or ImageNet [73, 72, 21]. SlowFast backbones: $T \times \tau = 8 \times 8$, R101. AVSlowFast shows strong margins (Δ) over SlowFast and previous state-of-the-art [41].

Inference. Following previous work [80, 16], we uniformly sample 10 clips from a video along its temporal axis. For each clip, we resize the shorter spatial side to 256 pixels and take 3 crops of 256×256 along the longer side to cover the spatial dimensions. Video-level predictions are computed by averaging softmax scores. We report the actual *inference-time* computation as in [16], by listing the FLOPs per spacetime “view” of spatial size 256^2 (temporal clip with spatial crop) at inference *and* the number of views (*i.e.* 30 for 10 temporal clips each with 3 spatial crops).

Kinetics, EPIC, Charades details are in A.4, A.5, & A.6.

4.1. Main Results

EPIC-Kitchens. We compare to state-of-the-art methods on EPIC in Table 2. First, AVSlowFast improves SlowFast by **+2.9 / +4.3 / +2.3** top-1 accuracy for verb / noun / action, which highlights the benefits of audio in egocentric video recognition. Second, as a system-level comparison, AVSlowFast exhibits higher performance in all three categories (verb/noun/action) and two test sets (seen/unseen) vs. state-of-the-art [41] under Kinetics-400 pretraining.

Comparing to LFB [82], which uses an object detector to localize objects, AVSlowFast achieves similar performance for nouns (objects) on both the seen and unseen test sets, whereas SlowFast *without audio* is largely lagging behind (-4.4% vs. LFB on val noun), which is intuitive as sound can be beneficial for recognizing objects.

We observe large performance gains over previous best [41] (which utilizes rgb, audio and flow) on the unseen split (*i.e.*, novel scenes) of the test set (**+3.1 / +4.8 / +2.3** for verb / noun / action), showing AVSlowFast’s strength on test data.

model	inputs	pretrain	top-1	top-5	KS	GFLOPs \times views
R(2+1)D [78]	V	-	72.0	90.0		152×115
TS R(2+1)D [78]	V+F	-	73.9	90.9		304×115
ECO [88]	V	-	70.0	89.4		$N/A \times N/A$
ip-CSN-152 [77]	V	-	77.8	92.8		109×30
S3D [84]	V	-	69.4	89.1		$66.4 \times N/A$
I3D [9]	V	\checkmark	72.1	90.3	N/A	$108 \times N/A$
TS I3D [9]	V+F	\checkmark	75.7	92.0		$216 \times N/A$
TS I3D [9]	V+F	-	71.6	90.0		$216 \times N/A$
Nonlocal [80], R101	V	\checkmark	77.7	93.3		359×30
S3D-G [84]	V	\checkmark	74.9	92.0		$71.4 \times N/A$
TS S3D-G [84]	V+F	\checkmark	77.2	93.0		$143 \times N/A$
3-stream SATT [8]	A+V+F	\checkmark	77.7	93.2		$N/A \times N/A$
SlowFast, R50 [16]	V	-	75.6	92.0	80.5	36×30
AVSlowFast , R50	A+V	-	77.0	92.7	83.7	40×30
SlowFast, R101 [16]	V	-	77.9	93.2	82.7	106×30
AVSlowFast , R101	A+V	-	78.8	93.6	85.0	129×30

Table 3. **AVSlowFast results on Kinetics.** AVSlowFast and SlowFast instantiations are with $T \times \tau = 4 \times 16$ and $T \times \tau = 8 \times 8$ inputs for R50/R101 backbones, without NL blocks. “TS” indicates Two-Stream. “KS” refers to top-1 accuracy on Kinetics-Sounds dataset [2]. “pretrain” refers to ImageNet pretraining.

model	pretrain	mAP	GFLOPs \times views
Nonlocal, R101 [80]	ImageNet+Kinetics	37.5	544×30
STRG, R101+NL [81]	ImageNet+Kinetics	39.7	630×30
Timeception [36]	Kinetics-400	41.1	$N/A \times N/A$
LFB, +NL [82]	Kinetics-400	42.5	529×30
SlowFast	Kinetics-400	42.5	234×30
AVSlowFast	Kinetics-400	43.7	278×30

Table 4. **Comparison with the state-of-the-art on Charades.** AV/SlowFast is with R101+NL backbone and 16×8 sampling.

Kinetics. Table 3 shows a comparison on the well-established Kinetics dataset. Comparing AVSlowFast with SlowFast shows a margin of 1.4% top-1 for R50 and 0.9% top-1 accuracy for R101, given the same network backbone and input size. This demonstrates the effectiveness of the audio stream despite its modest cost of only $\approx 10\%$ – 20% of the overall computation. Comparatively, going deeper from R50 to R101 increases computation by 194%.

On a system-level, AVSlowFast compares favorably to existing methods that utilize various modalities, *i.e.*, audio (A), visual frames (V) and optical flow (F). Adding optical flow streams brings roughly similar gains as audio but *doubles* computation (TS in Table 3), not counting optical flow computation; by contrast, audio processing is lightweight (*e.g.* 11% computation overhead for AVSlowFast, R50). Further, AVSlowFast does not rely on pretraining and is competitive with multi-modal approaches that pretrain individual modality streams (\checkmark).

As Kinetics is a visual-heavy dataset (for many classes *e.g.* “writing” audio is not useful), to better study audio-visual learning, “Kinetics-Sounds” [2] is as a subset of 34 classes potentially manifested both visually and aurally. We test on Kinetics-Sounds in the “KS” column of Table 3. The gain from SlowFast to AVSlowFast doubled – for R50/R101 with $+3.2\%/+2.3\%$, showing the potential on relevant data. Further Kinetics results on standalone Audio-only classification and class-level analysis are in A.2 and A.3.

connection	top-1	top-5	GFLOPs	β_A	top-1	top-5	GFLOPs	P_d	top-1	top-5	AVS	top-1	top-5
A→F→S	75.3	91.8	51.4	1/8	76.0	92.5	36.0	-	75.2	91.8	-	76.4	92.5
A→FS	77.0	92.7	39.8	1/4	76.6	92.7	36.8	0.2	76.0	92.5	res ₅	76.7	92.8
AV Nonlocal	77.2	92.9	39.9	1/2	77.0	92.7	39.8	0.5	76.7	92.7	res _{4,5}	76.9	92.9
				1	75.9	92.4	51.9	0.8	77.0	92.7	res _{3,4,5}	77.0	92.7

(a) Audiovisual fusion.

(b) Audio channels β_A .(c) DropPathway rate P_d .

(d) AV synchronization.

Table 5. **Ablations on AVSlowFast design** on Kinetics-400. We show top-1/5 classification accuracy (%), and computational complexity measured in GFLOPs for a single clip input of spatial size 256^2 . Backbone: 4×16 , R-50.

Charades. We test the effectiveness of AVSlowFast on videos of longer range activities on Charades in Table 4. We observe that audio can facilitate recognition (+1.2% over a strong SlowFast baseline) and we achieve state-of-the-art performance under Kinetics-400 pre-training.

Discussion. Overall, our experiments on action classification indicate that, on standard, visually created datasets for classification, a consistent improvement over very strong visual baselines can be achieved by modeling audio with AVSlowFast. For some cases improvements are exceptionally high (e.g. EPIC) and in some lower (e.g. Charades), and all results suggest that with AVSlowFast, audio can serve as an *economical* modality that supplements visual input.

4.2. Ablation Studies

We ablate of our approach on Kinetics as it represents the largest unconstrained dataset for human action recognition.

fusion stage	top-1	top-5	GFLOPs
SlowFast	75.6	92.0	36.1
SlowFast+Audio	76.1	92.0	-
pool ₅	75.4	92.0	38.4
res ₄ + pool ₅	76.5	92.6	39.1
res _{3,4} + pool ₅	77.0	92.7	39.8
res _{2,3,4} + pool ₅	75.8	92.4	40.2

Table 6. **Effects of hierarchical fusion.** Backbone: 4×16 , R-50.

Hierarchical fusion. We study the effectiveness of fusion in Table 6. The first interesting phenomenon is that direct ensembling (late-fusion) of audio/visual models produces only modest gains (76.1% vs 75.6%), whereas joint training with late-fusion (“pool₅”) does not help (75.6% → 75.4%).

For hierarchical, multi-level fusion, Table 6 shows it is beneficial to fuse audio and visual features at multiple levels. Specifically, we found that recognition accuracy steadily increases from 75.4% to 77.0% when we increase the number of fusion connections from one (i.e., only concatenating pool₅ outputs) to three (res_{3,4} + pool₅) where it peaks. Adding another lateral connection at res₂ decreases accuracy. This suggests that it is beneficial to start fusing audio and visual features from intermediate levels (res₃) all the way to the top of the network. We hypothesize that this is because audio facilitates the formation of visual concepts, but only when features mature to intermediate concepts that are generalizable across modalities (e.g. local edges do not have a general sound pattern).

Lateral connections. We ablate the the effect of different types of lateral connections between audio and visual pathways in Table 5a. First, A→F→S, which enforces strong temporal alignment between audio and visual streams, produces lower classification accuracy compared to A→FS, which relaxes the requirement on alignment. This is consistent with findings in [41] that it is beneficial to have tolerance on alignment between the modalities, since class-level audio signals might happen out-of-sync to visual frames (e.g., when shooting 3 pointers in basketball, the net-touching sound only comes after the action finishes). Finally, the straightforward A→FS connection performs similarly to the more complex AV Nonlocal [80] fusion (77.0% vs 77.2%). We use A→FS as our default lateral connection for its good performance and simplicity.

Audio pathway capacity. We study the impact of the number of channels of the Audio pathway (β_A) in Table 5b. As expected, when we increase the number of channels (e.g., increasing β_A from 1/8 to 1/2, which is the ratio between Audio and Slow pathway’s channels), accuracy improves at the cost of increased computation. However, performance starts to degrade when we further increase it to 1, likely due to overfitting. We use $\beta_A = 1/2$ across all our experiments.

DropPathway. We apply Audio pathway dropping to adjust the incompatibility of learning speed across modalities. Here we conduct ablative experiments to study the effects of different drop rates P_d . The results are shown in Table 5c. As shown in the table, a high value of P_d (0.5 or 0.8) is required to slow down the Audio pathway when training audio and visual pathways jointly. If we train AVSlowFast without DropPathway (“-”), the accuracy degrades to be even worse than visual-only models (75.2% vs 75.6%). This is because the Audio pathway learns too fast and starts to dominate the visual feature learning. The gain from 75.2% → 77.0% reflects the full impact of DropPathway.

Hierarchical audiovisual synchronization. We study the effectiveness of hierarchical audiovisual synchronization in Table 5d. We use AVSlowFast with and without AVS, and vary the layers for multiple losses. We observe that adding AVS as an auxiliary task is beneficial (+0.6% gain). Furthermore, having synchronization loss at multiple levels slightly increases the performance (without extra inference cost). This suggests that it is beneficial to have a feature representation that is generalizable across audio and visual modalities and hierarchical AVS could facilitate producing such.

model	inputs	AVA	pretrain	val mAP	GFLOPs
I3D [28]	V+F			15.6	N/A
ACRN, S3D [75]	V+F			17.4	N/A
ATR, R50+NL [38]	V+F			21.7	N/A
9-model ensemble [38]	V+F			25.6	N/A
I3D+Transformer [26]	V			25.0	N/A
LFB, + NL R50 [82]	V	v2.1	K400	25.8	N/A
LFB, + NL R101 [82]	V			26.8	N/A
SlowFast 4×16, R50	V			24.3	65.7
AVSlowFast 4×16, R50	A+V			25.4	67.1
SlowFast 8×8, R101	V			26.3	184
AVSlowFast 8×8, R101	A+V			27.8	210
SlowFast 4×16, R50	V			24.7	65.7
AVSlowFast 4×16, R50	A+V	v2.2	K400	25.9	67.1
SlowFast 8×8, R101	V			27.4	184
AVSlowFast 8×8, R101	A+V			28.6	210

Table 7. **Comparison on AVA detection.** AVSlowFast and SlowFast use 8×8 inputs. For R101, both use NL blocks [80].

5. Experiments: AVA Action Detection

In addition to the action classification tasks, we also apply AVSlowFast models on action detection which requires both localizing and recognizing actions.

Dataset. The AVA dataset [28] focuses on spatiotemporal localization of human actions. Spatiotemporal labels are provided for one frame per second, with people annotated with a bounding box and (possibly multiple) actions. There are 211k training and 57k validation video segments. We follow the standard protocol [28] of evaluating on 60 classes. The metric is mean Average Precision (mAP) over 60 classes, using a frame-level IoU threshold of 0.5.

Detection architecture. We follow the detection architecture introduced in [16], which is adapted from Faster R-CNN [62] for video. During training, the input to our audiovisual detector is $\alpha_F T$ RGB frames sampled with temporal stride τ and spatial size 224×224 , to SlowFast pathways, and the corresponding log-mel-spectrogram covering this time window to Audio pathway. During testing, the backbone feature is computed fully convolutionally with RGB frame of shorter side being 256 pixels [16], as is standard in Faster R-CNN [62].

For details on architecture, training and inference, please refer to appendix A.7.

Results. We compare to several other existing methods in Table 7. AVSlowFast, with both R50 and R101 backbones, outperforms SlowFast with a consistent margin of $\sim 1.2\%$, and only increases FLOPs² slightly, *e.g.* for R50 by only 2%, whereas going from SlowFast R50 to R101 (without audio) increases computation significantly by 180%.

Interestingly, the ActivityNet Challenge 2018 [24] hosted a separate track for multiple modalities, but no team could achieve gains using audio information on AVA data.

²We report FLOPs for fully-convolutional inference of a clip with 256×320 spatial size for SlowFast and AVSlowFast models, full test-time computational cost for these models is directly proportional to this.

method	inputs	#param	FLOPs	pretrain	UCF	HMDB
Shuffle&Learn [54, 74]	V	58.3M	N/A	K600	26.5	12.6
3D-RotNet [39, 74]	V	33.6M	N/A	K600	47.7	24.8
CBT [74]	V	N/A	N/A	K600	54.0	29.5
AVSlowFast	A+V	38.5M	63.4G	K400	77.4	42.2

Table 8. **Comparison using the linear classification protocol.** We only train the last fc layer after SSL pretraining AVSlowFast features on Kinetics. Top-1 accuracy averaged over three splits is reported. Backbone: $T \times \tau = 8 \times 8$, R50.

Our result shows, for the first time, that audio can be beneficial for action detection, where spatiotemporal localization is required, even with low computation overhead of just 2%.

For system-level comparison to other approaches, Table 7 shows that AVSlowFast achieves state-of-the-art performance on AVA under Kinetics-400 pretraining.

For comparisons with future work, we show results on the newer v2.2 of AVA, which provides updated annotations. We see consistent results as for v2.1. As for per-class results, we found classes like [“swim” +30.2%], [“dance” +10.0%], [“shoot” +8.6%], and [“hit (an object)” +7.6%] has the largest gain from audio; please see appendix A.3 and Fig. A.1 for more details.

6. Experiments: Self-supervised Learning

To further study the generalization of AVSlowFast models, we apply it to self-supervised learning (SSL). The goal here is not to propose a new SSL pretraining task. Instead, we are interested in how well a self-supervised video representation can be learned with AVSlowFast using existing tasks. We use the audiovisual synchronization [2, 46, 58] and image rotation prediction [25] (0° , 90° , 180° , 270° ; as a four-way softmax-classification) losses as pretraining tasks. With the learned AVSlowFast weights, we then retrain the last fc layer of AVSlowFast on UCF101 [69] and HMDB51 [47] following standard practice to evaluate the SSL feature representation. Table 8 lists the results. Using off-the-shelf pretext tasks, our smallest AVSlowFast, R50 model compares favorably to state-of-the-art SSL approaches on both datasets, with an absolute margin of **+23.4** and **+12.7** top-1 accuracy over previous best CBT [74]. This is highlighting the strength of the architecture, and the features learned by AVSlowFast. For more details and results, please refer to appendix A.1.

7. Conclusion

This work has presented AVSlowFast Networks, an architecture for integrated audiovisual perception. We show the effectiveness of the AVSlowFast representation with state-of-the-art performance on six datasets for video action classification, detection, and self-supervised learning tasks. We hope that AVSlowFast, as a unified audiovisual backbone, will foster further research in video understanding.

A. Appendix

A.1. Results: Self-supervised Learning

method	inputs	#param	FLOPs	pretrain	UCF	HMDB
Shuffle&Learn [54, 74]	V	58.3M	N/A	K600	26.5	12.6
3D-RotNet [39, 74]	V	33.6M	N/A	K600	47.7	24.8
CBT [74]	V	N/A	N/A	K600	54.0	29.5
AVSlowFast 4×16	A+V	38.5M	36.2G	K400	76.8	41.0
AVSlowFast 8×8	A+V	38.5M	63.4G	K400	77.4	42.2
AVSlowFast 16×4	A+V	38.5M	117.9G	K400	77.4	44.1
ablation (split1)						
SlowFast 4×16 (ROT)	V	33.0M	34.2G	K400	71.9	42.0
AVSlowFast 4×16 (AVS)	A+V	38.5M	36.2G	K400	73.2	39.5
AVSlowFast 4×16	A+V	38.5M	36.2G	K400	77.0	40.2

Table A.1. **Comparison using the linear classification protocol.** We only train the the last fc layer after self-supervised pretraining on Kinetics-400 (abbreviated as K400). Top-1 accuracy averaged over three splits is reported when comparing to previous work (top), results on split1 is used for ablation (bottom). All SlowFast models use use R50 backbones with $T \times \tau$ sampling.

In this section, we provide more results and detailed analysis on self-supervised learning using AVSlowFast. Training schedule and details are provided in §A.8.

First, we pretrain AVSlowFast with self-supervised objectives of audiovisual synchronization [2, 46, 58] (AVS) and image rotation prediction [25] (ROT) on Kinetics-400. Then, following the standard linear classification protocol used for image recognition tasks [30], we use the pretrained network as a fixed, *frozen* feature extractor and train a linear classifier on top of the self-supervisedly learned features. In Table A.1 (top), we compare to previous work that follows the *same protocol*. We note this is the same experiment as in Table 8, but with additional ablations on our models. The results indicate that features learned by AVSlowFast are significantly better than baselines including the recently introduced CBT method [74] (+23.4% for UCF101 and +14.6% for HMDB51), which also uses ROT as well as a contrastive bidirectional transformer (CBT) loss by pretraining on the larger Kinetics-600.

In addition, we also ablate the contribution of individual tasks of AVS and ROT in Table A.1 (bottom). On UCF101, SlowFast/AVSlowFast trained under either ROT or AVS objective show strong individual performance, while the combination of them perform the best. Whereas on the smaller HMDB51, all three variants of our method perform similarly well and audio seems less important.

Another aspect is that, although many previous approaches on self-supervised feature learning focus on reporting number of parameters, the FLOPs are another important factor to consider – as shown in Table A.1 (top), the performance keeps increasing when we take higher temporal resolution clips by varying $T \times \tau$ (*i.e.* larger FLOPs), even though model *parameters remain identical*.

Although we think the linear classification protocol

method	inputs	#param	pretrain	UCF101	HMDB51
Shuffle & Learn [54]	V	58.3M	UCF/HMDB	50.2	18.1
OPN [49]	V	8.6M	UCF/HMDB	59.8	23.8
O3N [19]	V	N/A	Kinetics-400	60.3	32.5
3D-RotNet [39]	V	33.6M	Kinetics-400	62.9	33.7
3D-ST-Puzzle [43]	V	33.6M	Kinetics-400	65.8	33.7
DPC [29]	V	32.6M	Kinetics-400	75.7	35.7
CBT [74]	V	N/A	Kinetics-600	79.5	44.6
Multisensory [58]	A+V	N/A	Kinetics-400	82.1	N/A
AVTS [45]	A+V	N/A	Kinetics-400	85.8	56.9
VGG-M motion [67, 18]	V	90.7M	-	83.7	54.6
AVSlowFast	A+V	38.5M	Kinetics-400	87.0	54.6

Table A.2. **Comparison for Training all layers.** Results using the popular protocol of fine-tuning all layers after self-supervised pretraining. Top-1 accuracy averaged over three splits is reported. We use AVSlowFast 16×4, R50 for this experiment. While this protocol has been used in the past, we think it is suboptimal for evaluation of self-supervised representations, as the training of all layers can significantly impact performance; *e.g.* an AlexNet-like VGG-M motion stream [67, 18] can perform among state-of-the-art self-supervised approaches, without any pretraining.

serves as a better method to evaluate self-supervised feature learning (as features are frozen and therefore less sensitive to hyper-parameter settings such as learning schedule and regularization, especially when these datasets are relatively small), we also evaluate by fine-tuning all layers of AVSlowFast on the target datasets to compare to a larger corpus of previous work on self-supervised feature learning. Table A.2 shows that AVSlowFast achieves competitive performance comparing to prior work under this setting. When using this protocol, we believe it is reasonable to also consider methods that train multiple layers on UCF/HMDB from scratch, such as optical-flow based motion streams [67, 18]. It is interesting that this stream, despite being an AlexNet-like model [11], is comparable or better, than many newer models, pretrained on (the large) Kinetics-400 using self-supervised learning techniques.

A.2. Results: Audio-only Classification

To understand the effectiveness of our Audio pathway, we evaluate it in terms of Audio-only classification accuracy on Kinetics (in addition to Kinetics-400, we also train and evaluate on Kinetics-600 to be comparable to methods that use this data in challenges [24]). In Table A.3, we compare our Audio-only network to several other audio models. We observe that our Audio-only model performs better than existing methods by solid margins (+3.3% top-1 accuracy on Kinetics-600 and +3.2% on Kinetics-400, compared to best-performing methods), which demonstrates the effectiveness of our Audio pathway design. Note also that unlike some other methods in Table A.3, we train our audio network from scratch on Kinetics, without any pretraining.

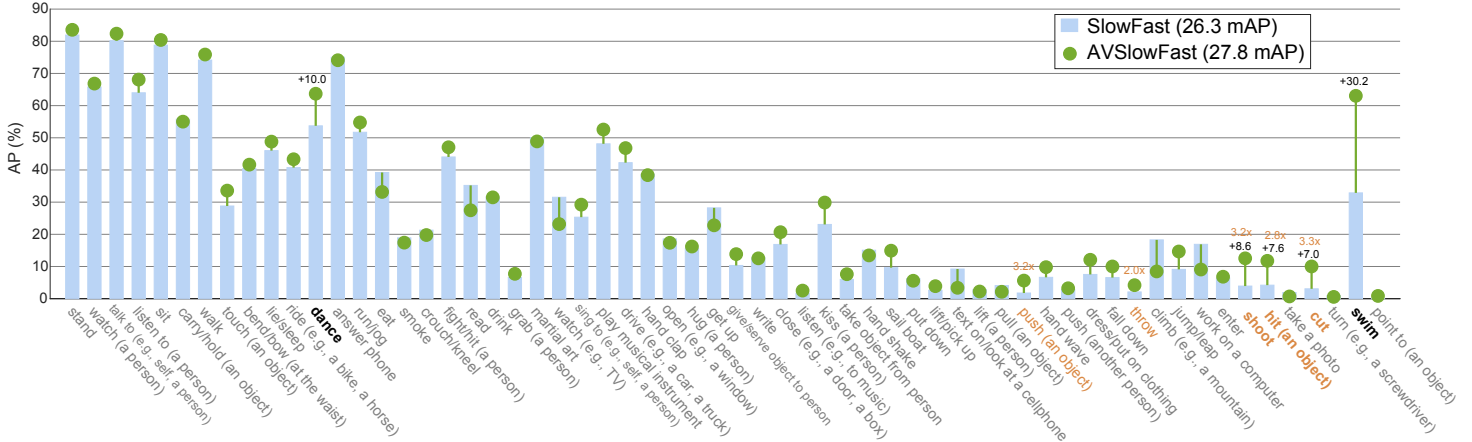


Figure A.1. AVA per-class average precision. AVSlowFast (27.8 mAP) vs. its SlowFast counterpart (26.3 mAP). The highlighted categories are the 5 highest absolute increases (**bold**) and top 5 relative increases over SlowFast (**orange**). Best viewed in color with zoom.

model	dataset	pretrain	top-1	top-5	GFLOPs
VGG* [32]	Kinetics-600	Kinetics-400	23.0	N/A	N/A
SE-ResNext [24]	Kinetics-600	ImageNet	21.3	38.7	N/A
Inception-ResNet [24]	Kinetics-600	ImageNet	23.2	N/A	N/A
Audio-only (ours)	Kinetics-600	-	26.5	44.7	14.2
VGG [8]	Kinetics-400	-	21.6	39.4	N/A
Audio-only (ours)	Kinetics-400	-	24.8	43.3	14.2

Table A.3. Results of Audio-only models. VGG* model results are taken from “iTXN” submission from Baidu Research to ActivityNet challenge, as documented in this report [24].

A.3. Results: Classification & Detection Analysis

Per-class analysis on Kinetics Comparing AVSlowFast to SlowFast (77.0% vs. 75.6% for 4×16 , R50 backbone), classes that benefited most from audio include [“*dancing macarena*” +24.5%], [“*whistling*” +24.0%], [“*beatboxing*” +20.4%], [“*salsa dancing*” +19.1%] and [“*singing*” +16.0%], etc. Clearly, all these classes have distinct sound signatures to be recognized. On the other hand, classes like [“*skiing (not slalom or crosscountry)*” -12.3%], [“*triple jump*” -12.2%], [“*dodgeball*” -10.2%] and [“*massaging legs*” -10.2%] have the largest performance loss, as sound of these classes tend to be much less correlated the action.

Per-class analysis on AVA We compare per-class results of AVSlowFast to its SlowFast counterparts in Fig. A.1. As mentioned in the main paper, classes with largest absolute gain (marked with bold black font) are “*swim*”, “*dance*”, “*shoot*”, “*hit (an object)*” and “*cut*”. Further, the classes “*push (an object)*” (3.2 \times) and “*throw*” (2.0 \times) largely benefit from audio in relative terms (marked with orange font in Fig. A.1). As expected, all these classes have strong sound signature that are easy to recognize from audio. On the other hand, the largest performance loss arises for classes such as “*watch (e.g., TV)*”, “*read*”, “*eat*” and “*work on a computer*”, which either do not have a distinct sound signa-

ture (“*read*”, “*work on a computer*”) or have strong background noise sound (“*watch (e.g., TV)*”). We believe explicitly modeling foreground and background sound might be a fruitful future direction to alleviate these challenges.

A.4. Details: Kinetics Action Classification

We train our models on Kinetics from scratch without any pretraining. Our training and testing closely follows [16]. We use a synchronous SGD optimizer and train with 128 GPUs using the recipe in [27]. The mini-batch size is 8 clips per GPU (so the total mini-batch size is 1024). The initial base learning rate η is 1.6 and we decrease it according to half-period cosine schedule [51]: the learning rate at the n -th iteration is $\eta \cdot 0.5[\cos(\frac{n}{n_{\max}}\pi) + 1]$, where n_{\max} is the maximum training iterations. We adopt a linear warm-up schedule [27] for the first 8k iterations. We use a scale jittering range of [256, 340] pixels for R101 model to improve generalization [16]. To aid convergence, we initialize all models that use Non-Local blocks (NL) from their counterparts that are trained without NL. We only use NL on res_4 (instead of $\text{res}_3+\text{res}_4$ used in [80]).

We train with Batch Normalization (BN) [37], and the BN statistics are computed within each 8 clips. Dropout [33] with rate 0.5 is used before the final classifier layer. In total, we train for 256 epochs (60k iterations with batch size 1024, for ~ 240 k Kinetics videos) when $T \leq 4$ frames, and 196 epochs when the Slow pathway has $T > 4$ frames: it is sufficient to train shorter when a clip has more frames. We use momentum of 0.9 and weight decay of 10^{-4} .

A.5. Details: EPIC-Kitchens Classification

We fine-tune from Kinetics pretrained AVSlowFast 8×8 , R101 (w/o NL) for this experiment. For fine-tuning, we freeze all BNs by converting them into affine layers. We train using a single machine with 8 GPUs. Initial base learn-

ing rate η is set to 0.01 and 0.0006 for verb and noun. We train with batch size 32 for 24k and 30k for verb and noun respectively. We use a step wise decay of the learning rate by a factor of $10\times$ at $2/3$ and $5/6$ of full training. For simplicity, we only use a single center crop for testing.

A.6. Details: Charades Action Classification

We fine-tune from the Kinetics pretrained AVSlowFast 16×8 , R101 + NL model, to account for the longer activity range of this dataset, and a per-class sigmoid output is used to account for the multi-class nature of the data. We train on a single machine (8 GPUs) for 40k iterations using a batch size of 8 and a base learning rate η of 0.07 with one $10\times$ decay after 32k iterations. We use a Dropout rate of 0.7. For inference, we temporally max-pool scores [80, 16]. All other settings are the same as those of Kinetics.

A.7. Details: AVA Action Detection

We follow the detection architecture introduced in [16], which is adapted from Faster R-CNN [62] for video. Specifically, we set the spatial stride of res_5 from 2 to 1, thus increasing the spatial resolution of res_5 by $2\times$. RoI features are then computed by applying RoIAlign [31] spatially and global average pooling temporally. These features are then fed to a per-class, sigmoid-based classifier for multi-label prediction. Again, we initialize from Kinetics pretrained models and train 52k iterations with initial learning rate η of 0.4 and batch size 16 (we train across 16 machines, so effective batch size $16\times 16=256$). We pre-compute proposals using an off-the-shelf Faster R-CNN person detector with ResNeXt-101-FPN backbone. It is pretrained on ImageNet and the COCO human keypoint data and more details can be found in [16, 82].

A.8. Details: Self-supervised Evaluation

For self-supervised pretraining, we train on Kinetics-400 for 120k iterations with per-machine batch size 64 across 16 machines and initial learning rate 1.6, similar to §A.4, but with step-wise schedule. The learning rate is decayed with $10\times$ three times at 80k, 100k and 110k iterations. We use linear warm-up (starting from learning rate 0.001) for the first 10k iterations. As noted in Sec. 6, we adopt the curriculum learning idea for audiovisual synchronization [45] to first train with easy negatives for the first 60k iterations and then switch to a mix of easy and hard negatives (1/4 hard, 3/4 easy) for the remaining 60k iterations. The easy negatives come from different videos, while hard negatives have a temporal displacement of at least 0.5 seconds.

For the “linear classification protocol” experiments on UCF and HMDB, we train 320k iterations (echoing [44], we found it beneficial to train long iterations in this setting) with an initial learning rate of 0.01, a half-period cosine decay schedule and a batch size of 64 on a single machine with

8 GPUs. For the “train all layers” setting, we train 80k / 30k iterations with batch size 16 (also on a single machine), an initial learning rate of 0.005 / 0.01 and a half-period cosine decay schedule, for UCF and HMDB, respectively.

B. Details: Kinetics-Sound dataset

The original 34 classes selected in [2] are based on an earlier version of the Kinetics dataset. Some classes are removed since then. Therefore, we use the following 32 classes that are kept in current version of Kinetics-400 dataset: “blowing nose”, “blowing out candles”, “bowling”, “chopping wood”, “dribbling basketball”, “laughing”, “mowing lawn”, “playing accordion”, “playing bagpipes”, “playing bass guitar”, “playing clarinet”, “playing drums”, “playing guitar”, “playing harmonica”, “playing keyboard”, “playing organ”, “playing piano”, “playing saxophone”, “playing trombone”, “playing trumpet”, “playing violin”, “playing xylophone”, “ripping paper”, “shoveling snow”, “shuffling cards”, “singing”, “stomping grapes”, “strumming guitar”, “tap dancing”, “tapping guitar”, “tapping pen”, “tickling”.

References

- [1] Huda Alamri, Chiori Hori, Tim K Marks, Dhruv Batra, and Devi Parikh. Audio visual scene-aware dialog (avsd) track for natural language generation in dstc7. In *DSTC7 at AAAI Workshop*, 2018. 2
- [2] Relja Arandjelovic and Andrew Zisserman. Look, listen and learn. In *ICCV*, 2017. 1, 2, 5, 6, 8, 9, 11
- [3] Relja Arandjelovic and Andrew Zisserman. Objects that sound. In *ECCV*, 2018. 1, 2, 5
- [4] John Arevalo, Thamar Solorio, Manuel Montes-y Gómez, and Fabio A González. Gated multimodal units for information fusion. *arXiv preprint arXiv:1702.01992*, 2017. 2
- [5] Yusuf Aytar, Carl Vondrick, and Antonio Torralba. Soundnet: Learning sound representations from unlabeled video. In *NIPS*, 2016. 1, 2, 5
- [6] Fabien Baradel, Natalia Neverova, Christian Wolf, Julien Mille, and Greg Mori. Object level visual reasoning in videos. In *ECCV*, 2018. 5
- [7] Lynne Bernstein, Edward Auer, Jintao Jiang, and Silvio Eberhardt. Auditory perceptual learning for speech perception can be enhanced by audiovisual training. *Frontiers in Neuroscience*, 2013. 3
- [8] Yunlong Bian, Chuang Gan, Xiao Liu, Fu Li, Xiang Long, Yandong Li, Heng Qi, Jie Zhou, Shilei Wen, and Yuanqing Lin. Revisiting the effectiveness of off-the-shelf temporal modeling approaches for large-scale video classification. *arXiv preprint arXiv:1708.03805*, 2017. 6, 10
- [9] Joao Carreira and Andrew Zisserman. Quo vadis, action recognition? a new model and the kinetics dataset. In *CVPR*, 2017. 6
- [10] Anna Llagostera Casanovas, Gianluca Monaci, Pierre Vandergheynst, and Remi Gribonval. Blind audiovisual source

- separation based on sparse redundant representations. *IEEE Transactions on Multimedia*, 2010. 2
- [11] K. Chatfield, K. Simonyan, A. Vedaldi, and A. Zisserman. Return of the devil in the details: Delving deep into convolutional nets. In *BMVC*, 2014. 9
- [12] Joon Son Chung, Andrew Senior, Oriol Vinyals, and Andrew Zisserman. Lip reading sentences in the wild. In *CVPR*, 2017. 2, 5
- [13] Joon Son Chung and Andrew Zisserman. Out of time: automated lip sync in the wild. In *ACCV*, 2016. 5
- [14] Dima Damen, Hazel Doughty, Giovanni Maria Farinella, Sanja Fidler, Antonino Furnari, Evangelos Kazakos, Davide Moltisanti, Jonathan Munro, Toby Perrett, Will Price, et al. Scaling egocentric vision: The epic-kitchens dataset. In *ECCV*, 2018. 2, 5
- [15] Ariel Ephrat, Inbar Mosseri, Oran Lang, Tali Dekel, Kevin Wilson, Avinatan Hassidim, William T Freeman, and Michael Rubinstein. Looking to listen at the cocktail party: A speaker-independent audio-visual model for speech separation. *arXiv preprint arXiv:1804.03619*, 2018. 2
- [16] Christoph Feichtenhofer, Haoqi Fan, Jitendra Malik, and Kaiming He. SlowFast Networks for Video Recognition. In *ICCV*, 2019. 2, 3, 4, 5, 6, 8, 10, 11
- [17] Christoph Feichtenhofer, Axel Pinz, and Richard Wildes. Spatiotemporal residual networks for video action recognition. In *NIPS*, 2016. 2
- [18] Christoph Feichtenhofer, Axel Pinz, and Andrew Zisserman. Convolutional two-stream network fusion for video action recognition. In *CVPR*, 2016. 5, 9
- [19] Basura Fernando, Hakan Bilen, Efstratios Gavves, and Stephen Gould. Self-supervised video representation learning with odd-one-out networks. In *CVPR*, 2017. 9
- [20] Akira Fukui, Dong Huk Park, Daylen Yang, Anna Rohrbach, Trevor Darrell, and Marcus Rohrbach. Multimodal compact bilinear pooling for visual question answering and visual grounding. *arXiv preprint arXiv:1606.01847*, 2016. 2
- [21] Antonino Furnari and Giovanni Maria Farinella. What would you expect? anticipating egocentric actions with rolling-unrolling LSTMs and modality attention. In *ICCV*, 2019. 6
- [22] Dhiraj Gandhi, Lerrel Pinto, and Abhinav Gupta. Learning to fly by crashing. In *IROS*, 2017. 2
- [23] R. Gao, R. Feris, and K. Grauman. Learning to separate object sounds by watching unlabeled video. In *ECCV*, 2018. 1, 2
- [24] Bernard Ghanem, Juan Carlos Niebles, Cees Snoek, Fabian Caba Heilbron, Humam Alwassel, Victor Escorcia, Ranjay Khristna, Shyamal Buch, and Cuong Duc Dao. The ActivityNet large-scale activity recognition challenge 2018 summary. *arXiv preprint arXiv:1808.03766*, 2018. 1, 2, 8, 9, 10
- [25] Spyros Gidaris, Praveer Singh, and Nikos Komodakis. Unsupervised representation learning by predicting image rotations. In *ICLR*, 2018. 8, 9
- [26] Rohit Girdhar, João Carreira, Carl Doersch, and Andrew Zisserman. Video Action Transformer Network. In *CVPR*, 2019. 8
- [27] Priya Goyal, Piotr Dollár, Ross Girshick, Pieter Noordhuis, Lukasz Wesolowski, Aapo Kyrola, Andrew Tulloch, Yangqing Jia, and Kaiming He. Accurate, large mini-batch SGD: Training ImageNet in 1 hour. *arXiv preprint arXiv:1706.02677*, 2017. 10
- [28] Chunhui Gu, Chen Sun, David A Ross, Carl Vondrick, Caroline Pantofaru, Yeqing Li, Sudheendra Vijayanarasimhan, George Toderici, Susanna Ricco, Rahul Sukthankar, et al. AVA: A video dataset of spatio-temporally localized atomic visual actions. In *CVPR*, 2018. 2, 5, 8
- [29] Tengda Han, Weidi Xie, and Andrew Zisserman. Video representation learning by dense predictive coding. In *ICCV Workshops*, 2019. 5, 9
- [30] Kaiming He, Haoqi Fan, Yuxin Wu, Saining Xie, and Ross Girshick. Momentum contrast for unsupervised visual representation learning. *arXiv preprint arXiv:1911.05722*, 2019. 9
- [31] Kaiming He, Georgia Gkioxari, Piotr Dollár, and Ross Girshick. Mask R-CNN. In *ICCV*, 2017. 11
- [32] Shawn Hershey, Sourish Chaudhuri, Daniel PW Ellis, Jort F Gemmeke, Aren Jansen, R Channing Moore, Manoj Plakal, Devin Platt, Rif A Saurous, Bryan Seybold, et al. CNN architectures for large-scale audio classification. In *ICASSP*, 2017. 10
- [33] Geoffrey E Hinton, Nitish Srivastava, Alex Krizhevsky, Ilya Sutskever, and Ruslan R Salakhutdinov. Improving neural networks by preventing co-adaptation of feature detectors. *arXiv preprint arXiv:1207.0580*, 2012. 10
- [34] Di Hu, Feiping Nie, and Xuelong Li. Deep multimodal clustering for unsupervised audiovisual learning. In *CVPR*, 2019. 2
- [35] Jinggang Huang and David Mumford. Statistics of natural images and models. In *CVPR*, 1999. 4
- [36] Noureldien Hussein, Efstratios Gavves, and Arnold WM Smeulders. Timeception for complex action recognition. In *CVPR*, 2019. 6
- [37] Sergey Ioffe and Christian Szegedy. Batch normalization: Accelerating deep network training by reducing internal covariate shift. *arXiv preprint arXiv:1502.03167*, 2015. 10
- [38] Jianwen Jiang, Yu Cao, Lin Song, Shiwei Zhang Yunkai Li, Ziyao Xu, Qian Wu, Chuang Gan, Chi Zhang, and Gang Yu. Human centric spatio-temporal action localization. In *ActivityNet Workshop on CVPR*, 2018. 8
- [39] Longlong Jing and Yingli Tian. Self-supervised spatiotemporal feature learning by video geometric transformations. *arXiv preprint arXiv:1811.11387*, 2018. 8, 9
- [40] Will Kay, Joao Carreira, Karen Simonyan, Brian Zhang, Chloe Hillier, Sudheendra Vijayanarasimhan, Fabio Viola, Tim Green, Trevor Back, Paul Natsev, et al. The kinetics human action video dataset. *arXiv preprint arXiv:1705.06950*, 2017. 2, 5
- [41] Evangelos Kazakos, Arsha Nagrani, Andrew Zisserman, and Dima Damen. EPIC-Fusion: Audio-Visual Temporal Binding for Egocentric Action Recognition. In *ICCV*, 2019. 1, 2, 4, 6, 7
- [42] Christian Keysers, Evelyne Kohler, M Alessandra Umiltà, Luca Nanetti, Leonardo Fogassi, and Vittorio Gallese. Au-

- diovisual mirror neurons and action recognition. *Experimental brain research*, 2003. 1, 2, 5
- [43] Dahun Kim, Donghyeon Cho, and In So Kweon. Self-supervised video representation learning with space-time cubic puzzles. In *AAAI*, 2019. 9
- [44] Alexander Kolesnikov, Xiaohua Zhai, and Lucas Beyer. Revisiting self-supervised visual representation learning. *arXiv preprint arXiv:1901.09005*, 2019. 11
- [45] Bruno Korbar, Du Tran, and Lorenzo Torresani. Cooperative learning of audio and video models from self-supervised synchronization. In *NIPS*, 2018. 2, 5, 9, 11
- [46] Bruno Korbar, Du Tran, and Lorenzo Torresani. SCSampler: Sampling salient clips from video for efficient action recognition. In *ICCV*, 2019. 5, 8, 9
- [47] Hildegard Kuehne, Hueihan Jhuang, Estibaliz Garrote, Tomaso Poggio, and Thomas Serre. HMDB: a large video database for human motion recognition. In *ICCV*, 2011. 5, 8
- [48] François Laurent, Mario Valderrama, Michel Besserve, Mathias Guillard, Jean-Philippe Lachaux, Jacques Martinerie, and Geneviève Florence. Multimodal information improves the rapid detection of mental fatigue. *Biomedical Signal Processing and Control*, 2013. 2
- [49] Hsin-Ying Lee, Jia-Bin Huang, Maneesh Singh, and Ming-Hsuan Yang. Unsupervised representation learning by sorting sequences. In *ICCV*, 2017. 9
- [50] Xiang Long, Chuang Gan, Gerard De Melo, Jiajun Wu, Xiao Liu, and Shilei Wen. Attention clusters: Purely attention based local feature integration for video classification. In *CVPR*, 2018. 2
- [51] Ilya Loshchilov and Frank Hutter. SGDR: Stochastic gradient descent with warm restarts. *arXiv preprint arXiv:1608.03983*, 2016. 10
- [52] Dominic W Massaro and Michael M Cohen. Tests of auditory–visual integration efficiency within the framework of the fuzzy logical model of perception. *The Journal of the Acoustical Society of America*, 2000. 1
- [53] Harry McGurk and John MacDonald. Hearing lips and seeing voices. *Nature*, 1976. 1
- [54] Ishan Misra, C Lawrence Zitnick, and Martial Hebert. Shuffle and learn: unsupervised learning using temporal order verification. In *ECCV*, 2016. 8, 9
- [55] Arsha Nagrani, Samuel Albanie, and Andrew Zisserman. Seeing voices and hearing faces: Cross-modal biometric matching. In *CVPR*, 2018. 2
- [56] Jiquan Ngiam, Aditya Khosla, Mingyu Kim, Juhan Nam, Honglak Lee, and Andrew Y Ng. Multimodal deep learning. In *ICML*, 2011. 2
- [57] Kei Omata and Ken Mogi. Fusion and combination in audio-visual integration. *Proceedings of the Royal Society A: Mathematical, Physical and Engineering Sciences*, 2007. 1
- [58] Andrew Owens and Alexei A Efros. Audio-visual scene analysis with self-supervised multisensory features. In *ECCV*, 2018. 1, 2, 5, 8, 9
- [59] Andrew Owens, Jiajun Wu, Josh H McDermott, William T Freeman, and Antonio Torralba. Ambient sound provides supervision for visual learning. In *ECCV*, 2016. 1, 2, 5
- [60] Gerasimos Potamianos, Chalapathy Neti, Guillaume Gravier, Ashutosh Garg, and Andrew W Senior. Recent advances in the automatic recognition of audiovisual speech. *Proceedings of the IEEE*, 2003. 2
- [61] Zhaofan Qiu, Ting Yao, and Tao Mei. Learning spatiotemporal representation with pseudo-3d residual networks. In *ICCV*, 2017. 2
- [62] Shaoqing Ren, Kaiming He, Ross Girshick, and Jian Sun. Faster R-CNN: Towards real-time object detection with region proposal networks. In *NIPS*, 2015. 8, 11
- [63] Daniel L Ruderman. The statistics of natural images. *Network: computation in neural systems*, 5(4):517–548, 1994. 4
- [64] Jean-Luc Schwartz, Frederic Berthommier, and Christophe Savariaux. Audio-visual scene analysis: evidence for a “very-early” integration process in audio-visual speech perception. In *International Conference on Spoken Language Processing*, 2002. 1
- [65] Arda Senocak, Tae-Hyun Oh, Junsik Kim, Ming-Hsuan Yang, and In So Kweon. Learning to localize sound source in visual scenes. In *CVPR*, 2018. 1, 2
- [66] Gunnar A. Sigurdsson, Gül Varol, Xiaolong Wang, Ali Farhadi, Ivan Laptev, and Abhinav Gupta. Hollywood in homes: Crowdsourcing data collection for activity understanding. In *ECCV*, 2016. 5
- [67] K. Simonyan and A. Zisserman. Two-Stream Convolutional Networks for Action Recognition in Videos. In *NIPS*, 2014. 2, 9
- [68] K. Simonyan and A. Zisserman. Very Deep Convolutional Networks for Large-Scale Image Recognition. In *ICLR*, 2015.
- [69] Khurram Soomro, Amir Roshan Zamir, and M Shah. A dataset of 101 human action classes from videos in the wild. *arXiv preprint arXiv:1212.0402*, 2012. 5, 8
- [70] Salvador Soto-Faraco, Daria Kvasova, Emmanuel Biau, Nara Ikumi, Manuela Ruzzoli, Luis Mors-Fernandez, and Mireia Torralba. *Multisensory Interactions in the Real World*. Elements in Perception. Cambridge University Press, 2019. 1
- [71] Barry E Stein. *The new handbook of multisensory processing*. MIT Press, 2012. 1
- [72] Swathikiran Sudhakaran, Sergio Escalera, and Oswald Lanz. FBK-HUPBA Submission to the EPIC-Kitchens 2019 Action Recognition Challenge. *arXiv preprint arXiv:1906.08960*, 2019. 6
- [73] Swathikiran Sudhakaran, Sergio Escalera, and Oswald Lanz. Hierarchical feature aggregation networks for video action recognition. *arXiv preprint arXiv:1905.12462*, 2019. 6
- [74] Chen Sun, Fabien Baradel, Kevin Murphy, and Cordelia Schmid. Contrastive bidirectional transformer for temporal representation learning. *arXiv preprint arXiv:1906.05743*, 2019. 8, 9
- [75] Chen Sun, Abhinav Shrivastava, Carl Vondrick, Kevin Murphy, Rahul Sukthankar, and Cordelia Schmid. Actor-centric relation network. In *ECCV*, 2018. 8
- [76] D. Tran, L. Bourdev, R. Fergus, L. Torresani, and M. Paluri. Learning spatiotemporal features with 3d convolutional networks. In *ICCV*, 2015. 2

- [77] Du Tran, Heng Wang, Lorenzo Torresani, and Matt Feiszli. Video classification with channel-separated convolutional networks. *arXiv preprint arXiv:1904.02811*, 2019. 6
- [78] Du Tran, Heng Wang, Lorenzo Torresani, Jamie Ray, Yann LeCun, and Manohar Paluri. A closer look at spatiotemporal convolutions for action recognition. In *CVPR*, 2018. 6
- [79] Limin Wang, Yuanjun Xiong, Zhe Wang, Yu Qiao, Dahua Lin, Xiaoou Tang, and Luc Van Gool. Temporal segment networks: Towards good practices for deep action recognition. In *ECCV*, 2016. 2
- [80] Xiaolong Wang, Ross Girshick, Abhinav Gupta, and Kaiming He. Non-local neural networks. In *CVPR*, 2018. 4, 6, 7, 8, 10, 11
- [81] Xiaolong Wang and Abhinav Gupta. Videos as space-time region graphs. In *ECCV*, 2018. 6
- [82] Chao-Yuan Wu, Christoph Feichtenhofer, Haoqi Fan, Kaiming He, Philipp Krahenbuhl, and Ross Girshick. Long-term feature banks for detailed video understanding. In *CVPR*, 2019. 6, 8, 11
- [83] Fanyi Xiao, Leonid Sigal, and Yong Jae Lee. Weakly-supervised visual grounding of phrases with linguistic structures. In *CVPR*, 2017. 2
- [84] Saining Xie, Chen Sun, Jonathan Huang, Zhuowen Tu, and Kevin Murphy. Rethinking spatiotemporal feature learning: Speed-accuracy trade-offs in video classification. In *ECCV*, 2018. 2, 6
- [85] B. Xiong, S. Jain, and K. Grauman. Pixel objectness: Learning to segment generic objects automatically in images and videos. *PAMI*, 2018. 5
- [86] Hang Zhao, Chuang Gan, Andrew Rouditchenko, Carl Vondrick, Josh McDermott, and Antonio Torralba. The sound of pixels. In *ECCV*, 2018. 2
- [87] Yuke Zhu, Roozbeh Mottaghi, Eric Kolve, Joseph J Lim, Abhinav Gupta, Li Fei-Fei, and Ali Farhadi. Target-driven visual navigation in indoor scenes using deep reinforcement learning. In *ICRA*, 2017. 2
- [88] Mohammadreza Zolfaghari, Kamaljeet Singh, and Thomas Brox. ECO: Efficient convolutional network for online video understanding. In *ECCV*, 2018. 6